

Numerical study of fast ion transport induced by MHD instabilities in the tokamak

M. Gobbin^a, P. Martin^a, L. Marrelli^a, H.-U. Fahrbach^b, M. Garcia-Muñoz^b, S. Günter^b,
V. Igochine^b, M. Maraschek^b, M. Reich^b, R.B. White^c and the AUG team

a) Consorzio RFX, Associazione ENEA-Euratom per la fusione, Padova, Italy

b) Max-Planck Institut für Plasmaphysik, Euratom-Association, Garching bei München, Germany

c) Princeton Plasma Physics Laboratory, Princeton, NJ, USA

In this paper we present the results of a numerical study of fast ion transport in a tokamak equilibrium perturbed by a MHD instability which produces a magnetic island, for example tearing modes or neoclassical tearing modes (NTM) [1]. This study is motivated by recent high-quality

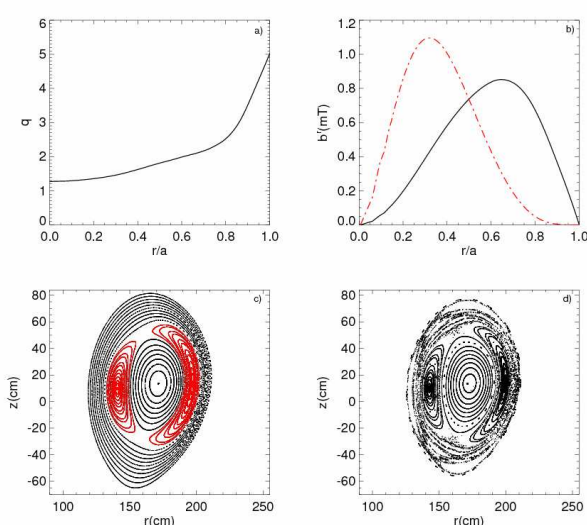


Figure 1

measurements of fast ion losses induced by NTMs and other MHD instabilities obtained in ASDEX-Upgrade [2], resolved both in pitch angle and energy [3]. These measurements provide a clear evidence of fast ion losses induced by (2,1) or (3,2) NTMs, which are well correlated with the phase and the amplitude of the instability.

The experimental findings are interpreted in the framework of a mechanism, which involves drift

islands in the fast particle orbit space [45]. The coupling between the fast particle guiding center motion in the perturbed magnetic field and the orbit shift due to the drift (which has a $(m=1, n=0)$ character and is relevant only for fast ions) results in several chains of drift islands in fast particle phase space. Depending on the shape of the q -profile, on the location of the resonance and on the amplitude of the original magnetic mode, these islands may or may not overlap, but in either case they may drive fast particle losses.

This mechanism has been initially studied by computing the trajectories of fast ions, injected by NBI in a simplified circular tokamak magnetic equilibrium perturbed by a (2,1) mode with the Hamiltonian guiding center code ORBIT [6]. Despite the simplification of the circular approach, the numerical simulation has captured several important aspects of the experimental results [3]. In order to improve the quality of the numerical simulation, we have developed a version of the code where the guiding center equations have been upgraded in order to deal with equilibria expressed in general straight field line flux coordinates. As a result, the constraint of Boozer coordinates, which was present in previous versions of the code, is relaxed. This, for example, allows using VMEC generated

equilibria, without coordinate conversion. In this paper the first results with the new approach are presented. A regular D-shaped AUG equilibrium is used, which refers to shot # 21089 at $t=2$ s. The corresponding safety factor q profile is reported in fig. 1-a. Superimposed on the equilibrium a stationary ($m=2, n=1$) magnetic perturbation has been considered, which is given by the formula $\mathbf{b}=\nabla \times \alpha \mathbf{B}$ where \mathbf{B} is the equilibrium magnetic field and

$$\alpha(\psi_p, \zeta, \theta) = \alpha_0 r(\psi_p)^m (\psi_p - \psi_{p,wall}) \sin(m\theta - n\zeta + \Phi) \tag{1}$$

where $r(\psi_p)$ is the normalized radius as a function of the poloidal flux, $\psi_{p,wall}$ is the poloidal flux at the wall, θ and ζ are the poloidal and toroidal angular coordinates respectively, and Φ is the mode

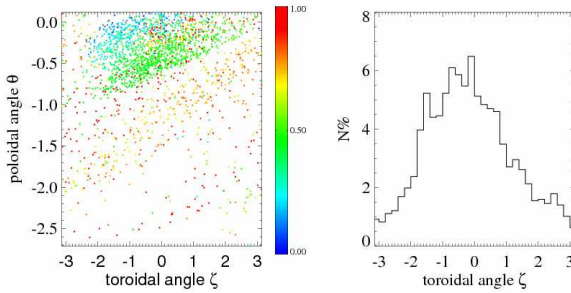


Figure 2

phase. The normalized radial profile of $b(r)$ is shown in fig. 1-b (solid curve). The resulting magnetic flux surfaces, with the (2,1) magnetic island, are displayed in fig. 1-c. The Poincaré puncture plot for the guiding center orbits of 93 keV (i.e. the energy of part of AUG NBI system) ions with velocity parallel to the magnetic field is shown in

Fig. 1-d, where the influence of multiple drift islands in producing a stochastic region can be observed. The initial fast ion population for ORBIT ($\approx 100,000$ particles) has been chosen as that resulting by the ionization pattern of the applied NBI sources in the experimental plasma [7]. Interactions of fast ions with the background plasma, i.e. pitch angle scattering and slowing down have been included.

The presence of the mode causes the enhancement of the fraction of fast particles reaching the wall in comparison with the unperturbed case, where only first orbit losses are present. The losses are mostly

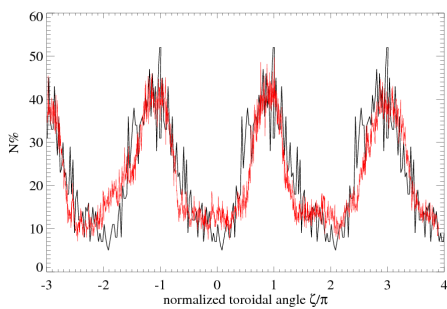


Figure 3

concentrated in a toroidally localized region and close to the equatorial mid plane, as shown by the distribution of the lost particles as a function of the toroidal angle reported in fig. 2-b: a single maximum is present, which is a signature of the $n=1$ character of the losses. In fig. 2-a a map of the loss locations of individual ions in the (θ, ζ) plane is reported (color coding indicates particles with different pitch, as shown in the scale).

Besides the $n=1$ feature, we note that most of the losses are concentrated around and just below the equatorial midplane. Both these features are consistent with the results previously observed in the circular case [3]; the agreement with experimental data is better, as expected, in the present D-shaped case, as shown in fig. 3. In this figure a few periods of one experimental signal

measuring the flux of lost ions have been superimposed on the simulated toroidal distribution (replicated several times) by mapping time into the toroidal angle, assuming a rotation with constant angular velocity and adjusting the initial phase to match the maximum. The amplitude of the signal is multiplied only by a constant without any change in the offset.

The amount of losses predicted by the code scales with the amplitude of the mode, i.e. with the width of the island, as also happens in the experiment. The numerical result is shown in Fig. 4, where we show the fraction of the lost ions vs. the amplitude of the magnetic perturbation.

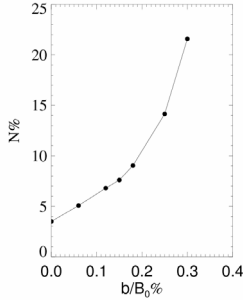


Figure 4

The distribution of loss times (defined as the time an ion takes to reach the wall), and of the energy and pitch angle the ions have when they are lost is discussed in fig.5. In particular the distribution of loss times of the ions is shown in fig.5-a. The distribution of the pitch angles is displayed in Fig. 5-b: this distribution is not flat, and shows that the effect of the magnetic island is such to cause losses preferentially around some pitch angles, consistent with the pattern experimentally observed in the scintillator [3]. In fig. 5-c is shown the distribution of the ion energy. The effect of slowing down is weak in time scales of the order of few ms, which are short in comparison with the slowing-down time (≈ 30 ms). In general we observe that ions with energy very close to their birth energy are lost

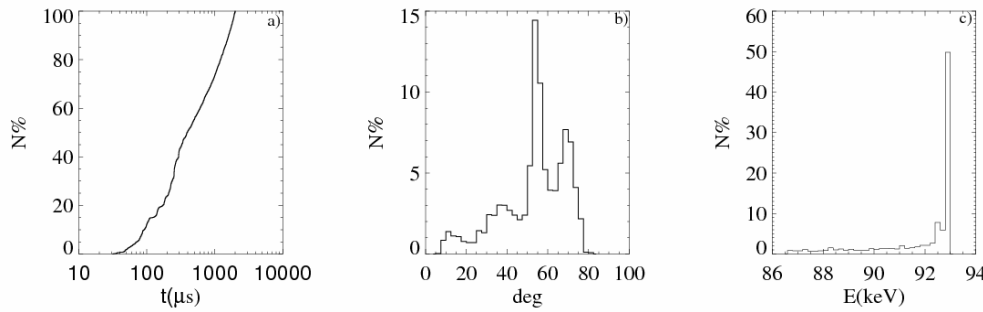


Figure 5

with
n a
rather
broad
range
of
times

starting from approximately 10 μ s up to time scales of the order of a few ms.

The amplitude of the original (2,1) magnetic perturbation at the resonant surface of the islands, which forms in the fast ion orbit space, for example the (3,1), influences the amount of losses, as well as the location of the (2,1) island O-point. To study this issue we have repeated the previous analysis using a different eigenfunction for the (2,1) mode, as that previously adopted in [8] and shown in fig 1-b (dashed curve) and expressed by:

$$\alpha(r, \xi, \theta) = \alpha_0 \left(\frac{r(\psi_p)}{x_0} \right)^m \left(\frac{1-r(\psi_p)}{1-x_0} \right)^{m(x_0^{-1}-1)} \sin(m\theta - n\xi + \Phi) \quad (2).$$

Where x_0 is an additional free parameter, which allows the control of the island O-point. This eigenfunction, for a given width of the (2,1) magnetic island, produces a smaller perturbation in

correspondence of the (3,1) rational surface in comparison with Eq. (1), as shown in Fig. 1-b. If we take a value of x_0 such that to displace the (2,1) island O-point by about 2 cm inward with respect to the previous case (which corresponds to the situation studied with the GORDON code [9]) the overall situations for the magnetic fields are not very different, but a more significant change is observed for the results obtained in the fast ion phase space. In fact, the perturbation of Eq. (2), while producing a similar magnetic island, causes less stochasticity in the fast ions orbit space.

This is shown in Fig. 6, which shows enlarged views of the Poincaré plot for the fast ions guiding center orbits around the midplane in the LFS. The frame of the left corresponds to the eigenfunction of Eq. (1), while that on the right to the eigenfunction of Eq. (2). As a result, the overall losses caused

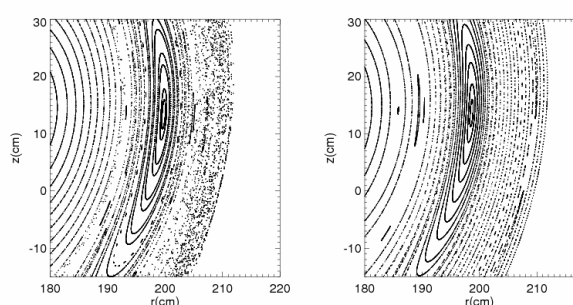


Figure 6

by the perturbation of Eq. (2) are significantly reduced. For example, for a magnetic island with a width of ≈ 11 cm, the losses due to the island decrease from a few percents of the injected ions to less than 0.3% when we move from a perturbation expressed by Eq. (1) to one expressed by Eq. (2). This result is qualitatively consistent with the results from the

GOURDON code [9], where an eigenfunction similar to (2) is being used.

In conclusion, the new version of the ORBIT code works reliably and significant extends the range of applications of this tool. Numerical simulations of the fast ion transport in presence of a magnetic island in a D-shaped geometry give results qualitatively consistent with previous numerical simulations in circular geometry, but now the numerical predictions are much closer to the experimental measurements. A sensitivity study on the detailed shape of the mode eigenfunction has been done, showing that the values of the magnetic perturbation at the rational surfaces influences fast ion losses. Further work will include the study of the effect on fast ion transport of islands with different geometrical helicity and amplitude (even simultaneously present in the plasma) and a detailed analysis of the influence of the magnetic ripple.

Acknowledgments: we thank Dr. E. Strumberger for the useful discussions.

This work was supported by the European Communities under the contract of Association between EURATOM/ENEA. The views and opinions expressed herein do not necessarily reflect those of the European Commission.

1 Chang Z. et al (1995) Phys. Rev. Lett. **74** 4663

2 Herrmann A. and Gruber O. (2003) Fusion Sci. Technol. **44** 569

3 M.Garcia-Muñoz et al., Nucl. Fusion (2007) **47** L10

4 Mynick H.E. (1993) Phys. Fluids **B 5** 1471

5 Zweben S.J. et al (1999) Nucl. Fusion **39** 1097

6 White R.B. (1984) Phys. Fluids **27** 2455

7 Lister G.G. (1985) Technical Report IPP 4/222, Max-Planck-Institut für Plasmaphysik, Garching

8 Carolipio E.M. et al (2002) Nucl. Fusion **42** 853

9 E. Strumberger (2007) private communication